

Sustainable stabilization of native subgrade soil for low-volume roads using copper slag and cementitious materials

Gunnam Sanijya ^{*,1, 2,a,b}, Bala Murugan R ^{1,c}, Samatha Chowdary P ^{2,d}

¹Annamalai University, Annamalai Nagar, Chidambaram 608002, India

²R V R & J C College of Engineering, Chowdavaram, Guntur 522019, Andhra Pradesh, India

Article Info

Article History:

Received 14 Feb 2025

Accepted 20 May 2025

Keywords:

Soil stabilization;
Copper slag;
Expansive soils;
Low-volume roads;
Geotechnical
properties;
Dynamic cone
penetration test

Abstract

The efficacy and longevity of low-volume roads (LVRs) are contingent upon the stabilization of native subgrade soil. This study aims to investigate the viability of using copper slag as a stabilizer when mixed with cementitious materials comprising lime and Ordinary Portland cement (OPC). Varying copper slag concentrations (2–12%) and a set 8% of lime or OPC were applied to expansive soil samples. Laboratory tests—including the California bearing ratio (CBR), unconfined compressive strength (UCS), and free swell index (FSI)—were used to determine swelling behavior, bearing capacity, and strength enhancement. The in-situ strength was evaluated using the Dynamic Cone Penetration Test (DCPT). The findings indicate that the incorporation of copper slag substantially enhanced the properties of the soil. UCS increased from approximately 53 kPa (untreated) to over 660 kPa for cement-stabilized soil (with 10% slag) and ~619 kPa for lime-stabilized soil. CBR (soaked) nearly doubled from 8% (at 2% slag) to 16% (at 10% slag). The swell potential was significantly diminished, with a reduction of up to 70% in cement–slag mixtures and 65% in lime–slag mixes in terms of FSI. Beyond the ideal copper slag level of about 8–10%, marginal strength increases or slight losses were noted. Cement-stabilized combinations outperformed lime-stabilized mixes in wet-dry durability and strength. Microstructural study (SEM) confirmed the development of a calcium-silicate-hydrate (C-S-H) gel, which improved particle bonding. DCPT penetration (DPI) and CBR ($R^2 = 0.90$) were found to have an exponential empirical correlation, which enables the estimation of in-situ strength. This study contributes to the sustainable development of rural road infrastructure by providing a cost-effective and environmentally favorable method for enhancing expansive subgrades through the inclusion of an industrial by-product.

© 2025 MIM Research Group. All rights reserved.

1. Introduction

Serving as the foundation layer for all subsequent layers, the subgrade soil is a key component of the pavement construction. Particularly on low-volume roads (LVRs), which carry light traffic yet may struggle with limited resources and suboptimal construction conditions, its stability and strength are crucial for the lifetime and use of pavements [1]. Expansive soils, a troublesome subgrade material, provide major problems because of their high shrink-swell potential, which causes pavement heaving and cracking. Seasonal moisture changes can lead to major pavement damage in areas where expansive clays prevail, thereby requiring efficient stabilization strategies [2,3]. Recent research emphasizes the influence of expansive soils on infrastructure and the requirement of creative treatment; for example, waste-to-energy ash and other industrial byproducts have been tested to treat very expansive clays in road pavements [4–6].

*Corresponding author: gsanijya24@gmail.com

^{a,b}orcid.org/0000-0002-4346-0985; ^corcid.org/0009-0003-0352-6139; ^dorcid.org/0000-0001-6668-2460

DOI: <http://dx.doi.org/10.17515/resm2025-682ma0214rs>

Res. Eng. Struct. Mat. Vol. x Iss. x (xxxx) xx-xx

Recent studies (2022–2025) show copper slag's promise in geotechnics. When mixed with lime or OPC, copper slag can significantly enhance the engineering qualities of expansive soils [7-10]. For instance, Jangid and Grover (2024) discovered that adding copper slag greatly strengthened and lowered the swell of an expansive clay, with around a 70% drop in free swell index at 30% slag concentration [11]. A mix of copper slag with hydrated lime and cement, according to Ekinici et al. (2022), improved the unconfined compressive strength of marine clay by as much as more pozzolanic processes and denser packing [12]. These investigations show the possibility of copper slag as a partial substitute for conventional stabilizers. Reflecting a more general movement toward sustainable binders, various industrial by-products such fly ash, ground-granulated blast furnace slag, and marble dust have also been studied for soil stabilization [13-17]. Combining copper slag with traditional binders can help to improve soil behavior specifically and usually at lower cost while also minimizing the environmental impact. Using copper slag in stabilization can help to balance some of the need for cement or lime, hence reducing energy consumption and CO₂ emissions linked with such binders [18-20].

Ensuring field performance and long-term durability is another facet of sustainable subgrade enhancement. Though they are vital, traditional lab tests—UCS, CBR, etc.—must be supplemented by field assessment methods [21]. Rapid evaluation of subgrade strength and compaction quality using the Dynamic Cone Penetration Test (DCPT) has proven to be a strong in-situ technique. Many recent research shows that pavement layer strength and CBR correspond strongly with DCPT findings, usually stated as Dynamic Penetration Index, DPI [22]. DCP can consistently reveal the strength of stabilized soils, according to Elias et al. (2023), hence it is a useful tool for field validation of laboratory findings [23]. Despite these developments, the literature still has gaps. Few studies have looked at copper slag with lime compared with cement on expansive soils in the setting of low-volume highways separately [24-26]. Furthermore, DCPT's application to assess such in situ stabilizations and development of region-specific correlations (DPI–CBR) remains constrained.

2. Research Significance and Novelty

This study offers fresh insights and suggests a sustainable stabilization technique to fill noted gaps considering the stated before. Unlike previous studies that tend to emphasize one stabilizer or combination additives, this one looks at two distinct binary mixing systems: (i) copper slag + lime, and (ii) copper slag + OPC. This lets one directly compare their effectiveness in treating expansive subgrade soil, which is new for low-volume road uses. A field correlation between DCPT and CBR is also created especially for the treated soil, hence enhancing empirical formulas from literature that might not apply to all soil types. Including a straightforward statistical modeling approach helps us to confirm the impact of copper slag amount and binder type on strength increases, therefore supporting the results even more. Overall, the study's novelty lies in its integrated approach: combining sustainable materials (industrial waste + minimal cement/lime) with field validation and statistical analysis to ensure the findings are both practical and generalizable.

In summary, this research contributes to sustainable infrastructure development by demonstrating that copper slag, an industrial waste, can be effectively used with traditional binders to stabilize expansive soils. It provides much-needed data on the performance of slag-lime vs. slag-cement stabilization, introduces a field evaluation correlation for immediate use by engineers, and employs statistical modeling to reinforce the trends observed. The following sections detail the materials and methods, present the results with in-depth discussion and comparative insights, and finally draw conclusions highlighting the study's novel contributions and practical implications.

3. Materials and Methods

3.1 Mix Proportions and Materials

The components for this investigation include ordinary Portland cement (OPC), hydrated lime, copper slag, and an expansive subgrade soil. Locally called as black cotton soil, the expansive soil was gathered at a depth of 2.5 m at Narkulapaadu village, Amaravati (Guntur district, India). High plasticity and swell potential characterize this soil. Classifying it as high-plasticity clay (CH) under

the Indian Standard system, the liquid limit is 52% and plasticity index 28.7%. A high expansiveness is confirmed by the free swell index (FSI) of 120%, which creates notable concerns for pavement stability. The physical and index characteristics of the soil are summarized in Table 1. Especially, the natural UCS of this soil is only approximately 53 kN/m² (about 53 kPa), indicating very poor strength, and it has a significant clay component (~82% clay-sized particles).

Table 1. Physical and engineering properties of soil

S.No	Property	Value
1	Specific gravity	2.55
2	Particle size distribution	
	a) Sand (%)	16.8
	b) Gravel (%)	0.9
	c) Clay (%)	82.3
3	Liquid limit (%)	52
4	Plastic limit (%)	22.42
5	Shrinkage limit (%)	8.6
6	IS classification of soil	CH
7	Plasticity index	28.72
8	Optimum moisture content (%)	36.24
9	Maximum dry density (kN/m ³)	13.4
10	Unconfined Compression test (kN/m ²)	52.97
11	Differential free swell index (%)	120

A commercial OPC (53 grade) complying to IS 269:2015 [27] was the cement utilized. Among its main characteristics (Table 2) are a fineness of 325 m²/kg, specific gravity of 3.04, initial setting time of 42 minutes, and 28-day compressive strength of about 59.4 MPa. A nearby supplier (Peduguralla Lime Factory) provided hydrated lime, a common high-calcium lime for soil stabilization.

Table 2. Physical properties of cement

Property	Value
Fineness (m ² /kg)	325
Specific Gravity	3.04
Initial Setting Time (minutes)	42
Compressive Strength (MPa)	59.4

The main sustainable component in this work is copper slag bought from Sterlite Industries in Tuticorin, India. A by-product of copper pyrometallurgy, copper slag is a black, glassy granular substance. The physical characteristics of the slag (Table 3) show that it is somewhat coarse (fineness modulus of 3.47, in the sand-sized range) and has a high specific gravity (3.5). Its bulk density (~1.91 g/cm³) is greater than that of normal soils, and it has low water absorption (0.4%) and moisture content (0.25%). Copper slag's angular particles can enhance soil gradation and friction; its latent silica and alumina might interact with lime or cement to generate more cementitious materials.

Table 3. Physical properties of copper slag

Property	Value
Specific Gravity	3.5
Fineness Modulus	3.47
Bulk Density (g/cm ³)	1.91
Water Absorption (%)	0.40
Moisture Content (%)	0.25

Mix designs were selected for stabilization depending on preliminary research and literature. Both lime and cement were chosen with a cementitious binder content of 8% (by dry soil weight) since 6–8% is a generally useful range for treating very plastic clays. To isolate the impact of copper slag, this % was maintained constant. Incremental percentages of 0%, 2%, 4%, 6%, 8%, 10%, and 12% copper slag were added (by dry soil weight). Binder-alone stabilization is based on the 0% slag scenario (soil + 8% binder only). Considering reasonable replacement levels and to see whether too much slag could be harmful—as some research indicate lower performance beyond an optimum point—the top limit of 12% slag was selected. Binder kind and slag concentration define each combination; e.g., "Lime + 8% slag" or "Cement + 10% slag".

3.2 Sample Preparation

Following ASTM D6913 [28], expansive soil clods were air-dried, pulverized, and sieved through a 4.75 mm sieve to remove gravel and big clods. The needed amounts of dry soil, copper slag, and binder—lime or cement—were weighed for each batch and dry-mixed until a consistent combination resulted. Optimum moisture content (OMC ~36%) water was progressively added to the dry mix during mixing, constantly swirling and kneading the substance. Preliminary tests using normal Proctor compaction (ASTM D698 [29]) revealed the OMC. Mixing kept going until the workable, uniform soil-binder-slag mix showed.

To shape the test specimens, materials were compacted right after mixing. Consistency with subgrade field compaction was achieved by compacting the slurry into cylindrical molds (38 mm diameter x 76 mm height) using a Standard Proctor energy (ASTM D698 [29]) for UCS specimens. This meant putting the mix in three layers and using 25 blows of a 2.5 kg rammer dropped from 300 mm for each layer. Using altered Proctor effort according to ASTM D1557 [30], CBR test samples were made in CBR molds (152 mm diameter x 178 mm height) to guarantee a high degree of compaction reflective of field circumstances (energy ~2,700 kN-m/m³). To prevent disruption, all specimens were meticulously extruded from molds following compression.

The compressed samples were cured in a humid atmosphere to gain strength. Stored in a curing chamber at about 27°C, each UCS sample was sealed in a plastic bag to stop moisture loss. Strength increases over time was evaluated using curing durations of 7, 14, and 28 days. This lets one see the pozzolanic reaction development, particularly for lime stabilization which is slower. Unless otherwise stated, specimens were soaked in water for approximately 4 hours to mimic worst-case field moisture conditions prior to testing. For CBR, designated samples were soaked for 96 hours to assess soaked CBR.

3.3 Testing Procedures

A suite of laboratory and field tests was performed to evaluate the stabilized soil's properties:

3.3.1 Unconfined Compressive Strength (UCS)

UCS tests were conducted in accordance with ASTM D2166/D2166M [31]. The cylindrical specimens were loaded axially at a strain rate of ~1% per minute until failure (Fig. 1 shows a schematic of the test setup). The peak load at failure was recorded, and UCS was computed as;

$$UCS = P/A \quad (1)$$

where P is the peak load and A is the cross-sectional area. UCS provides a measure of the soil's compressive strength without lateral confinement, indicating how well the stabilization improved the soil's load-bearing capacity. Cylindrical soil specimens (38 mm × 76 mm) are placed in a loading frame and compressed axially until failure. The maximum load is used to calculate the UCS.

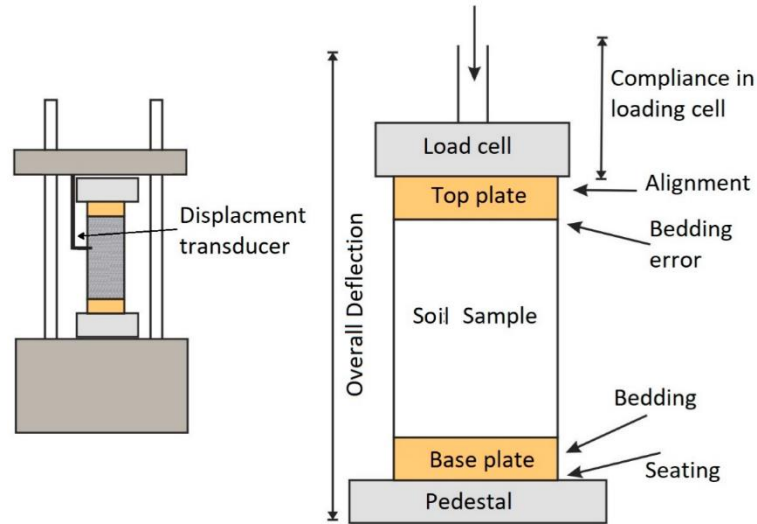


Fig. 1. UCS Test setup (schematic) [31]

3.3.2 California Bearing Ratio (CBR)

CBR tests were performed as per ASTM D1883 [32] to evaluate the stabilized soil's bearing capacity, which is critical for pavement design. Both unsoaked and soaked CBR were measured, but emphasis is on soaked CBR (96-hour soak) since subgrades often encounter wet conditions. After curing, samples in CBR molds were soaked (if required) and then penetrated with a standard piston (50 mm diameter) at 1.25 mm/min. The loads at 2.5 mm and 5.0 mm penetration were recorded. The CBR value is the ratio (in percentage) of the measured load to a standard load (1370 kg for 2.5 mm penetration). Fig. 2 shows the CBR test setup. Higher CBR indicates greater shearing resistance under a standard load, thus a more robust subgrade.

$$CBR\ Value = \frac{Measured\ Load}{Standard\ Load} \times 100 \quad (2)$$

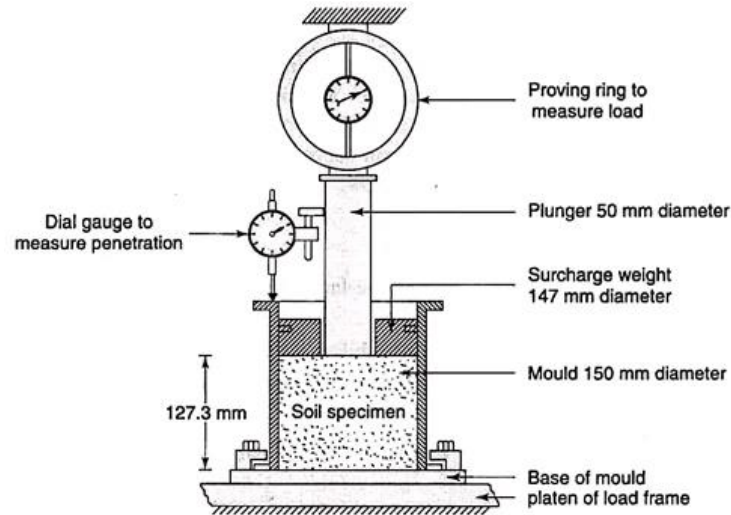


Fig 2. CBR Test Setup (schematic) [32]

3.3.3 Free Swell Index (FSI)

The free swell test (per ASTM D4829 [33]) quantifies the soil's swell potential when inundated. 10 g of oven-dry pulverized soil passing 425 μm sieve was used for each trial. The soil was poured into two graduated cylinders: one filled with distilled water and another with kerosene (non-polar liquid where clay doesn't swell). After 24 hours, the volumes in each cylinder were noted. FSI (%) was calculated as

$$FSI (\%) = \frac{V_w - V_k}{V_k} \times 100 \quad (3)$$

where V_w is the volume in water and V_k in kerosene. For stabilized soil, a reduction in FSI indicates that the treatment has inhibited the expansive clay minerals' ability to swell. Lower swell is desirable for subgrades to prevent pavement uplift. The test was done on powdered samples from cured and air-dried specimens for each mix to assess how stabilization reduced the inherent swell potential.

3.3.4 Dynamic Cone Penetration Test (DCPT)

The DCPT (also called DCP) was employed as a field test to assess in-situ strength of the stabilized soil layers. We followed ASTM D6951 [34] for test procedure. A pit (1 m × 1 m × 0.5 m) was prepared at the test site and backfilled with the stabilized soil mixture in layers, compacted to field density. The DCP apparatus consists of an 8 kg hammer dropping from 575 mm height onto an anvil that drives a 60° cone (20 mm base diameter) into the soil. The penetration after each blow (or set of blows) was recorded to calculate the Dynamic Penetration Index (DPI), typically reported in mm/blow. A higher DPI signifies softer ground (more penetration per blow), whereas a lower DPI indicates a stronger, more resistant soil. In our tests, DPI was recorded for each mix at the end of curing by performing DCP on the constructed test beds. The obtained DPI values were later used to estimate CBR via existing empirical correlations and to develop a project-specific correlation (see Section 4.4).

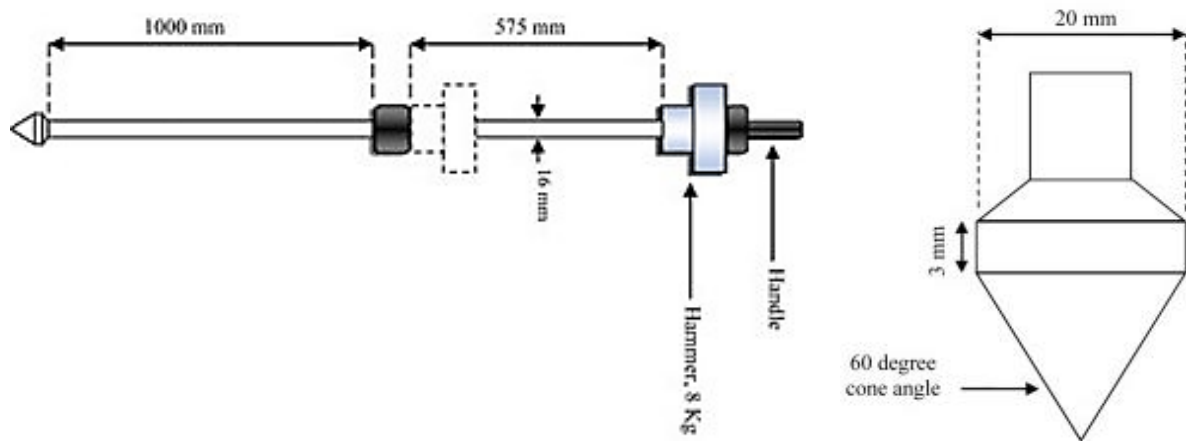


Fig. 3. Schematic of Dynamic Cone Penetration Test (DCPT) [34]

3.3.5 Durability (Wetting-Drying Cycles)

To evaluate the durability of stabilized soil under environmental stresses, wetting–drying (W-D) cycle tests were conducted (ASTM D559 [35]). Specimens stabilized with 8% binder and various slag contents were subjected to 12 cycles of alternate soaking (wetting) and oven-drying, simulating seasonal moisture fluctuations. Each cycle consisted of submerging the sample in water for 5 hours followed by oven drying at 60°C for 42 hours. After 12 cycles, the cumulative weight loss of each specimen was measured to assess material disintegration. In addition, UCS tests were performed after selected cycles (every 4 cycles) to see strength retention. This durability test indicates how well the stabilized soil can withstand repeated swelling and shrinkage—critical for long-term performance. Scanning Electron Microscopy (SEM) was also carried out on samples after 0, 4, 8, and 12 W-D cycles to observe microstructural changes (Section 4.5).

4. Results and Discussion

After curing and testing the various stabilized mixes, the results are presented and discussed in the following sub-sections. Unless stated otherwise, the discussed trends correspond to the 28-day cured samples, as they exhibited the highest strength and most stabilized behavior. All results for

lime-stabilized mixes (soil–lime–slag) are compared alongside those for cement-stabilized mixes (soil–OPC–slag) to highlight differences in performance. Wherever relevant, findings are contextualized with recent literature to underscore agreements or distinctions, thereby deepening the discussion.

4.1 Unconfined Compressive strength (UCS)

The UCS values of the stabilized soil showed a marked improvement with the addition of copper slag (Figure 4). The untreated soil had a UCS of only ~53 kPa (Table 1), which increased dramatically upon stabilization. With 8% binder alone (0% slag), the 28-day UCS reached around 380–420 kPa for lime and cement respectively (extrapolated from the 2% slag data trend). As copper slag content increased from 2% to 8%, UCS rose substantially for both binders. Cement-stabilized specimens exhibited higher strength gains compared to lime-stabilized ones at all equivalent slag contents. For instance, at the optimal 8% slag content, the UCS was about 600 kPa for the lime mix and 616–620 kPa for the cement mix. With 10% slag, UCS peaked at ~661 kPa for cement and ~619 kPa for lime (average values), reflecting roughly 50–65% strength gain over the 2% slag mixes (which were ~450 kPa and 400 kPa respectively). This indicates that copper slag provides additional strength beyond what the binder alone achieves, up to a point.

The initial rise in UCS with slag can be attributed to multiple factors. First, copper slag's high specific gravity and angular particles likely improved the packing density of the soil-binder matrix, thereby increasing the material's load-bearing capacity. Second, copper slag contains oxides of silicon, iron, and aluminum which, in the presence of lime or the calcium from cement hydration, can participate in secondary pozzolanic reactions. This leads to additional cementitious gel formation (such as C–S–H and C–A–H), binding soil particles more effectively. The microstructural analysis (Section 3.5) indeed confirmed the formation of C–S–H gels coating the particles in slag-amended mixes, especially at 8% slag where the structure was densest. Cement-based stabilization outperformed lime-based stabilization in UCS, particularly at early curing stages and lower slag contents, because OPC hydration provides an immediate supply of cementitious compounds (calcium hydroxide, calcium silicate hydrates) that strengthen the soil. Lime requires time to react with soil silica/alumina (a slower pozzolanic process), and thus lime-stabilized soils often gain strength more gradually. Kumar and Walia [16] have noted that lime's effect is time-dependent, improving plasticity and facilitating long-term strength, whereas cement yields more immediate strength gains.

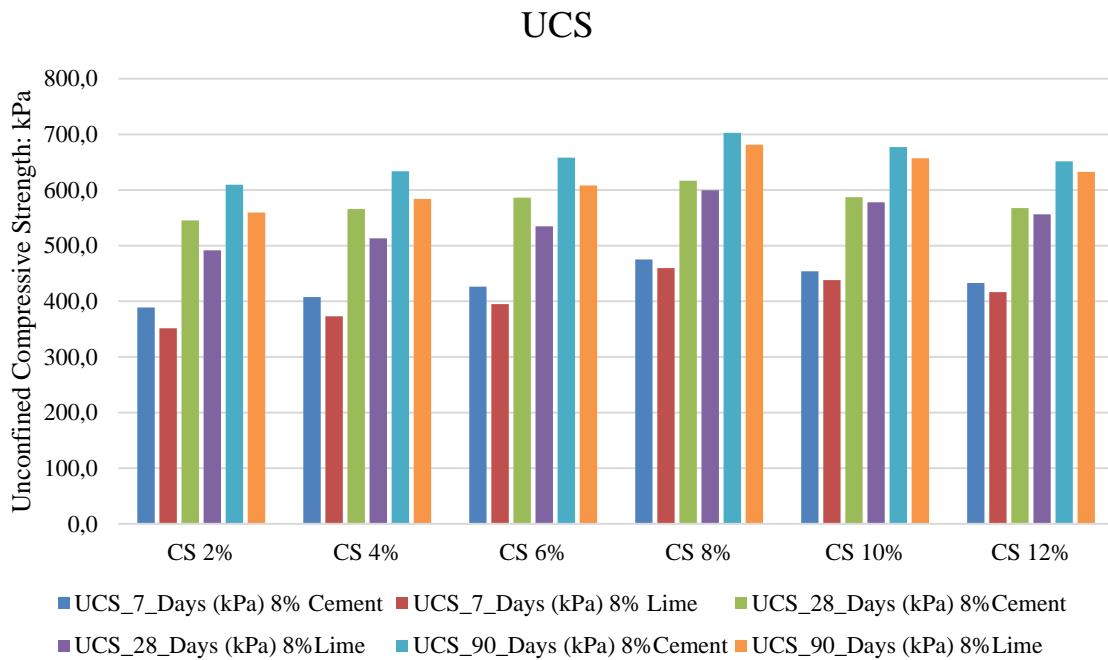


Fig. 4. UCS values for different proportions of copper slag and Cementitious materials

There appeared to be an optimum slag content around 8–10%. Beyond this, at 12% slag, the UCS did not increase further and in some cases showed a slight decrease (e.g., a marginal drop from 660 kPa at 10% slag to ~630 kPa at 12% slag for the cement mix, as inferred from Figure 4). This trend suggests that excessive slag might lead to diminishing or negative returns in strength. A plausible explanation is that at high slag content, not all slag particles can participate in bonding; instead, they may act as inert inclusions if insufficient binder is present to react with them. The surplus unreacted slag can create weak points or micro-voids in the matrix, slightly reducing strength. Similar findings were reported by Ekinci et al. (2022), who observed an optimal ratio of slag in a slag–lime–cement mix for peak strength, with too much slag causing a drop in UCS due to dilution of binder effectiveness. Therefore, while copper slag is beneficial, its content should be optimized relative to the binder amount. In our case, ~1 part binder to 1 part slag (8% each) was an optimal proportion for maximizing UCS.

4.2 California Bearing Ratio (CBR)

The CBR values of the stabilized soil followed trends similar to UCS, as expected, since both reflect soil strength. Figure 5 illustrates the soaked CBR for mixes with 8% binder (lime or cement) and varying slag. The native soil had a very low soaked CBR (<2%), typical of expansive clays that lose strength upon saturation. With stabilization, soaked CBR increased significantly. At 2% slag, the soil + 8% lime mix showed a CBR of about 4–5%, whereas soil + 8% cement showed around 6–8%. These base stabilized values (with minimal slag) were already improvements due to binder alone. As copper slag content increased to 8–10%, the CBR jumped markedly. The highest CBR recorded was about 16% for the cement-stabilized soil with 10% slag. The corresponding lime-stabilized mix had a CBR around 14–15% at 10% slag. In percentage terms, this is roughly a doubling of CBR from the low-slag cases (e.g., from ~8% at 2% slag to 16% at 10% slag in cemented mixes). Even 12% slag did not increase CBR further, indicating a leveling off. The unsoaked CBR (not shown in figure) were higher, as expected (roughly 1.5–2 times the soaked CBR), but since pavements are generally designed with soaked CBR for conservatism, our focus is on the soaked values.

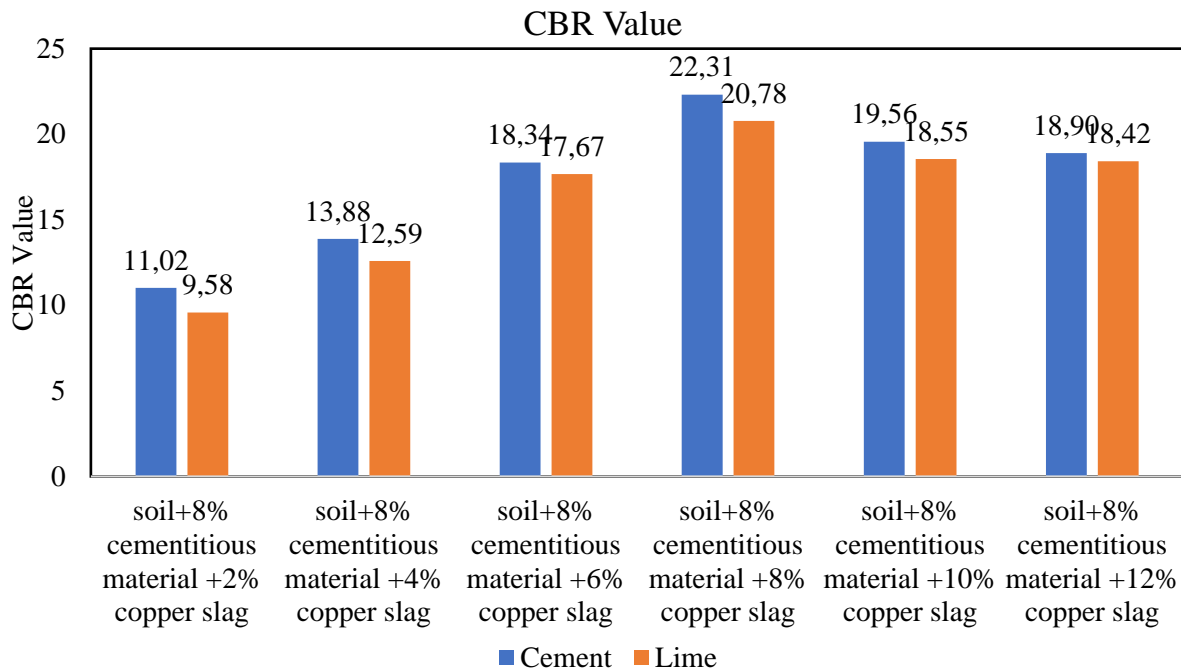


Fig. 5. CBR values of soil sample with optimum percentage of lime and cement and increasing percentage of copper slag

The enhancement in CBR with slag can be explained by improved particle interlock and shear resistance of the matrix. Copper slag particles act somewhat like a sand/gravel component in the soil, increasing the frictional stability under the penetrating piston. Moreover, the binding action of the cementitious products (from lime or cement reactions) with slag leads to a stiffer material that

resists penetration. It is noteworthy that cement+slag outperformed lime+slag in CBR as well, albeit modestly. At optimum slag, cement mix CBR was ~16% vs. lime mix ~14%. This aligns with the UCS results, since a higher UCS generally correlates with a higher CBR for a given soil type. Another observation is that beyond ~8–10% slag, the CBR did not substantially improve or may even decline slightly. This suggests an optimal point similar to UCS behavior. Additional slag beyond optimum may not contribute to bearing resistance proportionally and could even introduce excess fines that soften on soaking.

4.3 Free Swell Index (FSI)

The free swell index of the soil decreased dramatically upon stabilization (Table 4). The untreated soil's FSI was 120%, reflecting severe swelling potential. With the addition of 8% lime (no slag), the FSI dropped to around 50%, and with 8% cement (no slag) to about 40% (these can be inferred from the 2% slag entries in Table 5 as there is minimal slag effect at 2%). The inclusion of copper slag further suppressed the swelling. Each increment in slag content led to a lower FSI for both lime and cement mixes. At the optimum 8% slag, the FSI was reduced to 24% for the lime-stabilized soil and 19% for the cement-stabilized soil. These values represent an 80–85% reduction in swell potential compared to the original soil. Even at 12% slag, FSI went as low as ~15% with cement and ~20% with lime (meaning the expansive soil was practically converted to a non-expansive soil, as $FSI < 20\%$ is generally considered low expansiveness).

The greater efficacy of cement over lime in reducing FSI is evident but not as pronounced as in strength metrics. Both stabilizers achieved substantial swell reduction. Cement-stabilized soil's lower FSI can be attributed to the formation of cementitious compounds that bind clay particles and fill the voids, thereby restraining the soil from absorbing water and swelling. Lime also reduces swell by cation exchange and flocculation of clay particles (transforming them into more silt-like, non-expanding aggregates). However, lime's full impact on swell reduction can sometimes take longer to manifest, whereas our measurements were at 28 days. The addition of copper slag contributes to swell reduction in two ways: (1) Particle Replacement: slag particles (non-plastic) replace a portion of clay in the mix, directly reducing the amount of expansive clay present; (2) Pozzolanic Reaction: slag provides silica and alumina that, in presence of calcium (from lime or cement), form cementitious gels coating clay particles, which limits their expansion. The data indicates diminishing returns at higher slag contents (beyond ~8–10% slag, the FSI is already very low, so there's little swell left to eliminate). Notably, by 10–12% slag, the FSI values are nearly the same for both binders (~15–20%). This suggests a floor effect: once most clay is stabilized and excess voids are filled, the remaining slight swell might be due to pockets of untreated clay or micro-fissures on wetting, which neither additional slag nor a different binder can further reduce significantly. Achieving $<20\%$ FSI means the soil would pose minimal swelling problems in the field (comparable to an inert fill). This is a crucial outcome for the sustainability of pavements on such subgrades.

Table 4. Free Swell Index (FSI) of stabilized soil for varying copper slag content

Copper Slag (%)	FSI (%) with 8% Lime	FSI (%) with 8% Cement
0 (control)	50	40
2	30	25
4	28	23
6	26	21
8	24	19
10	22	17
12	20	15

Comparatively, Jangid and Grover observed ~70% reduction in swell with 30% copper slag alone [11]. Our study achieves a similar (~85%) reduction with a combination of lime/cement and much less slag, highlighting the efficiency of combined stabilization. Lime-fly ash mixtures in other studies also report significant swell reductions, reinforcing that proper admixtures can mitigate

expansive behavior [12-15]. The advantage of our copper slag approach is that it also contributes to strength, whereas some additives like only lime can reduce swell but not improve strength as much. Thus, the dual benefit of slag here is clear: it simultaneously increases strength and reduces swell, which is ideal for treating expansive subgrades.

4.4 Dynamic Cone Penetration (DCP) Test results

Field DCP tests were performed on both lime-stabilized and cement-stabilized pads with varying slag content. The results are summarized in Table 5 in terms of the Dynamic Penetration Index (DPI), which is the penetration per hammer blow (mm/blow). Lower DPI indicates a stronger (more resistant) soil. The general trend observed was that increasing copper slag content up to 8% reduced the DPI (thus improved the strength), while beyond 8%, the DPI slightly increased, especially for the lime-treated soil.

Table 5. Dynamic penetration index (DPI) for different mixes (after 28 days curing)

Copper Slag (%)	DPI (mm/blow) – Cement-stabilized	DPI (mm/blow) – Lime-stabilized
0 (8% binder only)	45.01	50.02
2	35.89	40.77
4	27.66	30.12
6	20.97	22.66
8	16.80	19.51
10	19.13	21.90
12	23.19	26.57

At 8% slag, the cement-stabilized pad achieved a DPI of 16.8 mm/blow, whereas the lime-stabilized pad had 19.5 mm/blow. These low DPI values correspond to a well-compacted, strong subgrade (for reference, a DPI <20 is usually associated with CBR well above 10% in many soils). The minimum DPI occurred at 8% slag for both binders, indicating peak strength, which aligns with the UCS/CBR optimum. When slag content was raised to 10% and 12%, DPI values increased (meaning penetration resistance dropped a bit). This again mirrors the slight drop in UCS/CBR at higher slag, showing consistency between lab and field indicators. Cement-treated soil consistently showed lower DPI (higher strength) than lime-treated soil at the same slag content, affirming the superior performance of cement noted earlier. To utilize the DCP results for practical evaluation, we compared the predicted CBR from existing empirical correlations with the actual CBR from lab tests. Several established equations relate DPI (or DCP penetration rate) to CBR; some examples are listed in Table 6. We applied these correlations to our DPI data (Table 7 shows an excerpt of predicted vs. experimental CBR for key mixes). It was found that existing correlations did not accurately predict our CBR values – predictions often deviated significantly, sometimes overestimating, or underestimating CBR especially for the lime-stabilized case. This is likely because those correlations were developed for different soil types or aggregate bases and may not directly apply to a stabilized expansive clay. For instance, Patel and Patel (2012) gave $CBR = 24.903 \cdot (DPI)^{-1.331}$; using our DPI, this tended to over-predict CBR for low DPI (strong soils).

Table 6. Correlation equations developed for CBR and DPI by previous researchers

S. No.	Author/s	Material Type	Correlation equation
1.	Gabr et al. [36]	Mixture of fine-grained soil and granular material	$\text{Log CBR} = 1.55 - 0.55 \text{ Log (DPI)}$
2.	Webster et al. [37]	Granular and cohesive materials	$\text{Log CBR} = 2.465 - 1.12 \text{ Log (DPI)}$
3.	Mejias Santiago et al. [38]	High compressible clay	$\text{CBR} = 442.92 / (DPI)^{1.119}$
4.	Patel and Patel [39]	Clay soils and silty sands	$\text{CBR} = 24.903(DPI)^{-1.331}$

Table 7. Predicting CBR values from DCP Index values using different empirical relations

Copper Slag (%)	Soil + Cement + Copper Slag						Soil + Lime + Copper Slag					
	Exp. CBR	Predicted CBR Values					Exp. CBR	Predicted CBR Values				
		[35]	[36]	[37]	[38]	[39]		[35]	[36]	[37]	[38]	[39]
2	11.02	5.29	4.95	1.82	8.06	0.21	9.58	4.59	4.62	2.13	6.99	0.18
4	13.88	7.09	5.71	1.31	10.79	0.30	12.59	6.44	5.45	1.46	9.81	0.27
6	18.34	9.66	6.65	0.93	14.70	0.43	17.67	8.86	6.38	1.02	13.48	0.39
8	22.31	12.39	7.52	0.70	18.85	0.58	20.78	10.48	6.92	0.85	15.94	0.48
10	19.56	10.71	7.00	0.83	16.30	0.49	18.55	9.21	6.50	0.98	14.01	0.41
12	18.90	8.63	6.30	1.05	13.14	0.38	18.42	7.41	5.84	1.25	11.28	0.32

Due to these discrepancies, we established a new empirical relationship tailored to our data. Figure 6 plots the experimentally measured CBR (soaked) against the corresponding DPI for all mixes. A clear inverse relationship is observed: as DPI decreases, CBR increases. We fitted various regression models (linear, power, exponential) to the data and found that an exponential model best described the CBR–DPI relationship for our stabilized soil. The correlation can be expressed as;

$$\text{CBR} = 367.12 \text{ DPI}^{-0.973} \quad (4)$$

The development of this site-specific correlation is a valuable outcome. It means that for similar soil and stabilization, one can quickly perform a DCP test in the field and estimate the subgrade's CBR using the above formula, without waiting for lab CBR tests. This is especially useful for quality assurance during construction of LVRs: if the DPI measured on compacted stabilized layers is below a threshold (e.g., 20 mm/blow), the correlation assures that the CBR (and hence subgrade support) is satisfactory (e.g., >13–15%). Our findings echo those of Lee et al. (2019), who emphasized that instrumented DCP can reliably assess subgrade strength in situ [23]. By refining the correlation for expansive soil stabilization, we contribute a practical tool for engineers dealing with such materials.

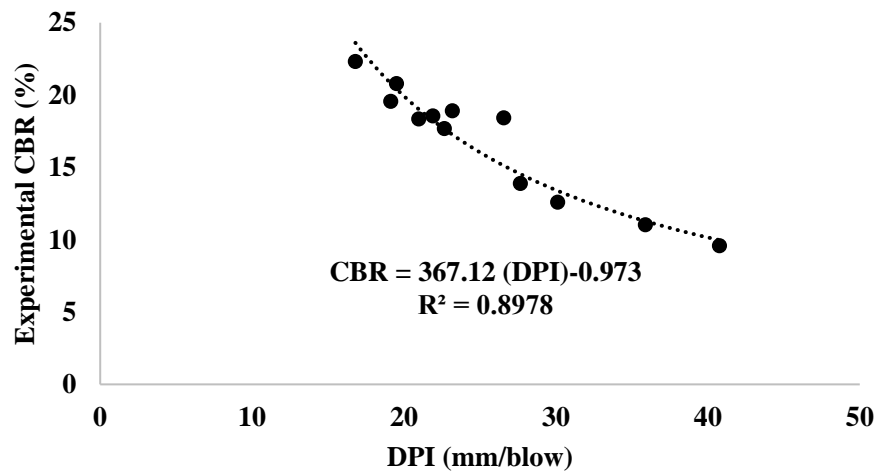


Fig 6. Correlation between DPI and experimental CBR

In summary, the DCPT results and the derived correlation reinforce the laboratory findings and add confidence that the improvements in soil properties (strength and stiffness) translate to field conditions. Cement-stabilized slag mixes show slightly better field performance than lime mixes, and the optimal slag content of ~8% is confirmed in the field by minimum DPI (maximum strength). The new DPI–CBR curve fills an important gap for field assessment, as previous generic correlations were unsuitable for our case. Future projects in similar soil environments can adopt this approach to verify stabilization effectiveness quickly on-site.

4.5 Microstructural Analysis (SEM)

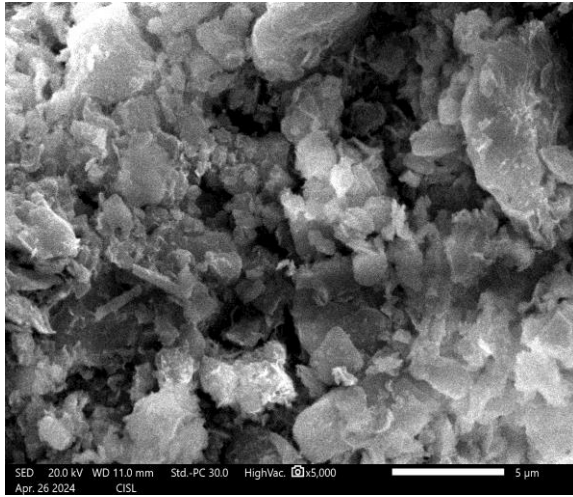
Scanning Electron Microscopy was performed on selected stabilized soil samples to observe the micro-level changes due to the additives. Figure 7 (a–f) and Figure 8 (a–f) present secondary electron SEM images for soil mixed with 8% lime + various slag contents, and soil with 8% cement+various slag contents, respectively. The magnifications used (on the order of 1000–2000×) allowed us to identify particle bonding, fabric arrangement, and the presence of cementitious reaction products.

In the lime-stabilized series (Fig. 7), the untreated soil (not shown here) exhibited a loose fabric with clay platelets having a face-to-face orientation and significant inter-particle voids. With 2% slag + 8% lime (Fig. 7a), we start to see clay particles coated with thin reaction products and slag particles embedded in the matrix but not fully bonded. There are still considerable voids and a fragmented structure. By 8% slag + 8% lime (Fig. 7d), the micrograph reveals a much denser matrix: clay particles and slag are bonded by a web of cementitious gel (C–S–H and C–A–H). The structure is cohesive, with slag particles acting as nodes around which the gel has formed. This corresponds to the optimum mix where macroscopically we saw peak strength and lowest swell. At higher slag (Fig. 7f for 12% slag + lime), some unreacted slag particles are noticeable – appearing as dark, angular bodies not tightly covered by gel – and micro-cracks can be seen around them, indicating a point of potential weakness. This supports the idea that beyond optimum slag, the surplus may not integrate well into the matrix.

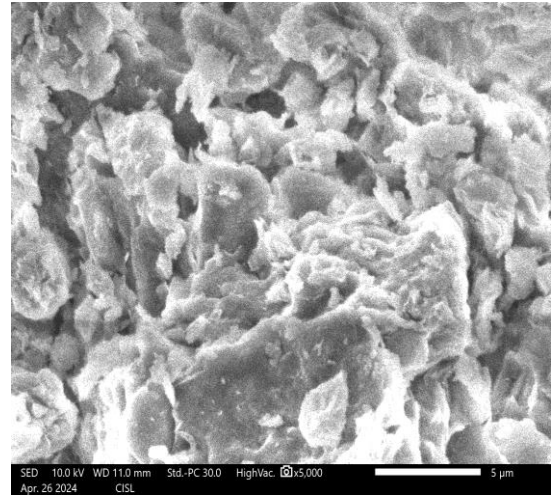
In the cement-stabilized series (Fig. 8), the images similarly show progressive densification up to an optimal slag content. 2% slag + 8% cement (Fig. 8a) already shows significant cementitious material binding the soil (since cement hydrates readily even without slag). The addition of slag introduces additional surfaces for C–S–H to form, and some slag appears partially hydrated (edges of particles slightly eroded, suggesting reaction). At 8% slag + 8% cement (Fig. 8d), the microstructure is very dense and uniform. The pores are filled with reaction products, and the slag particles are well bonded, effectively becoming part of a load-bearing skeleton. This image had the most tightly knit fabric among all, reflecting why this mix gave top performance. At 12% slag + 8% cement (Fig. 8f), similar to the lime case, a few voids and unreacted particle surfaces are apparent. The matrix is still solid, but one can discern areas where excessive slag led to pockets not fully cemented.

Overall, the SEM analysis confirms the mechanism of stabilization: the formation of cementitious gels (like C–S–H) from the reaction of calcium (from lime/cement) with silica/alumina (from soil and slag) is clearly evident. These gels are the binding agent that glue soil particles and slag together, transforming the soft clay into a firmer, aggregated structure. The optimal slag content (~8%) achieved a balance where enough slag was present to maximize these reactions and densify the matrix, but not so much as to leave unreacted excess. At this optimum, C–S–H crystals were observed abundantly, imparting rigidity and strength. The micrographs also explain the reduced FSI: in stabilized samples, clay particles are no longer free; they are encapsulated by or fused with cementitious products. This restrains the clay from swelling independently. We saw very few discrete clay platelets in the treated samples; most were part of larger cemented clusters.

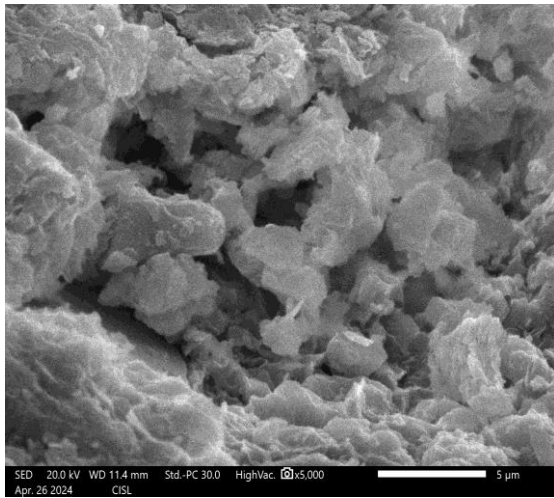
The comparative microstructure between lime and cement mixes indicates that cement mixes had a slightly more coherent matrix at earlier stages (due to rapid hydration). Lime mixes, while eventually also forming substantial cementitious bonding (especially with slag's pozzolanic action), may have more heterogeneous distribution of products initially. This could be one reason the lime mixes needed more curing time to catch up in strength. Nonetheless, by 28 days and optimal mix, both showed a qualitatively similar dense structure. These microscopic observations strongly correlate with the macroscopic test results, lending confidence to our understanding of why and how copper slag and cementitious binders improved the soil.



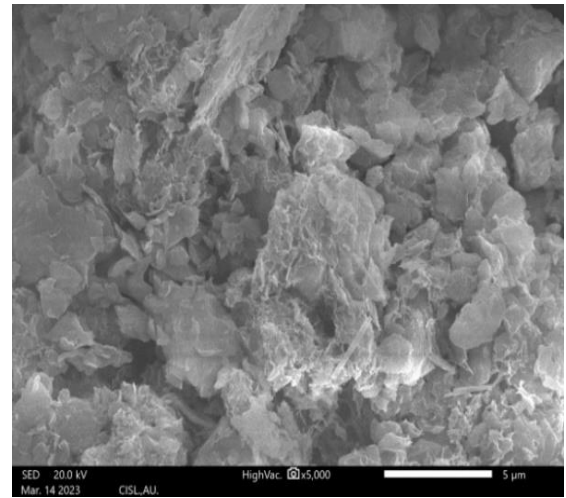
(a)



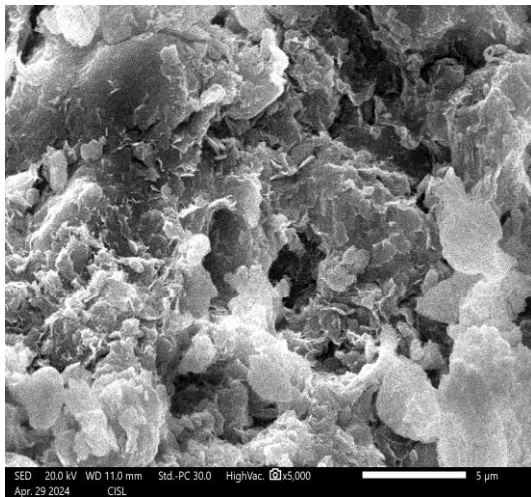
(b)



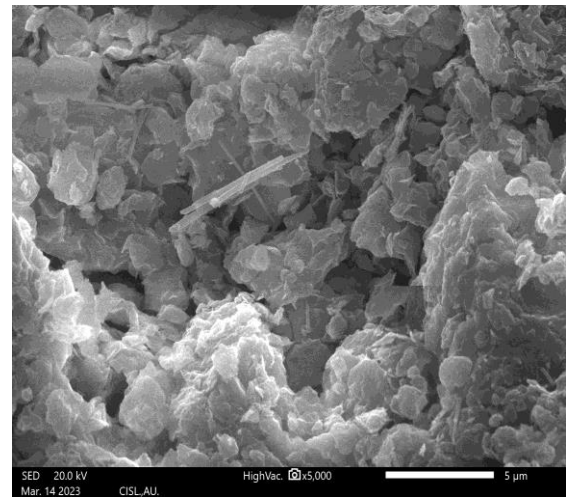
(c)



(d)

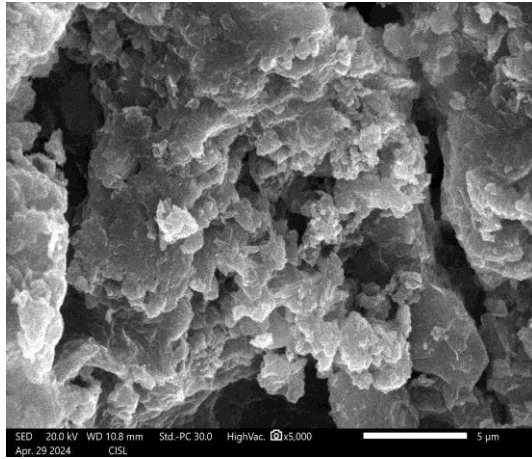


(e)

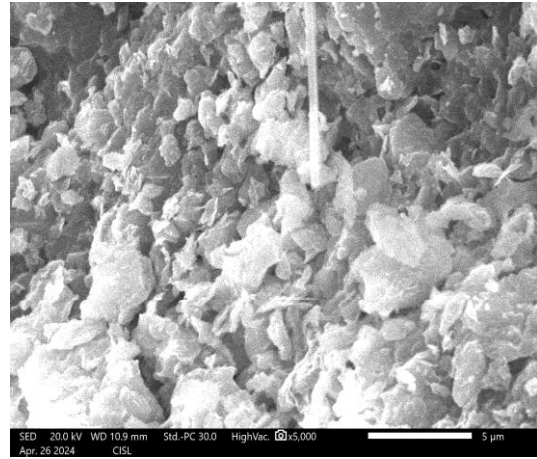


(f)

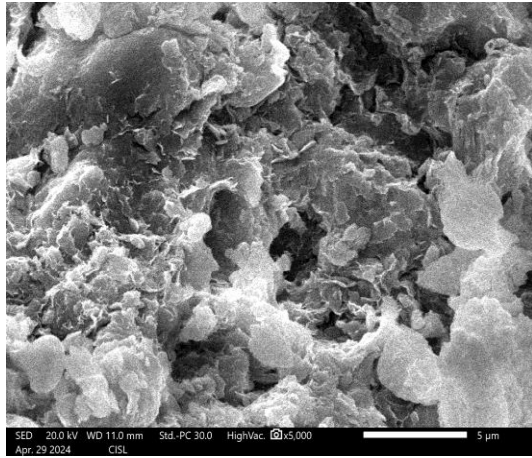
Fig. 7. Microstructural images (SEM) of soil samples stabilized with lime + copper slag (a) Soil + 8% lime with 2% slag, (b) Soil + 8% lime with 4% slag, (c) Soil + 8% lime with 6% slag, (d) Soil + 8% lime with 8% slag, (e) Soil + 8% lime with 10% slag and (f) Soil + 8% lime with 12% slag



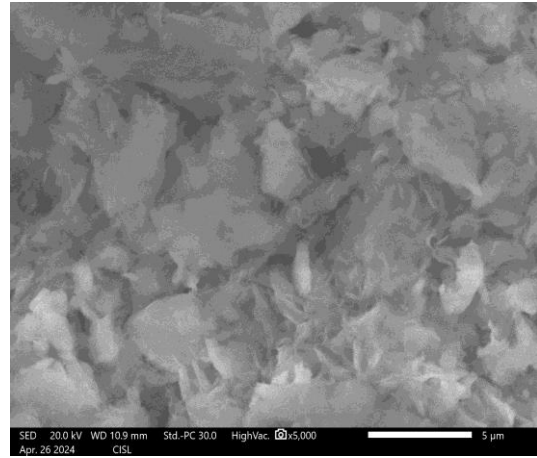
(a)



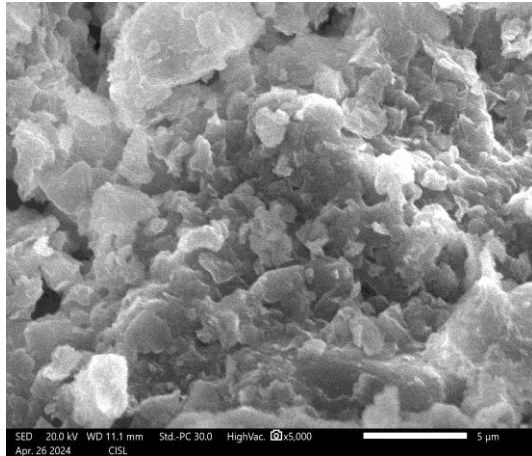
(b)



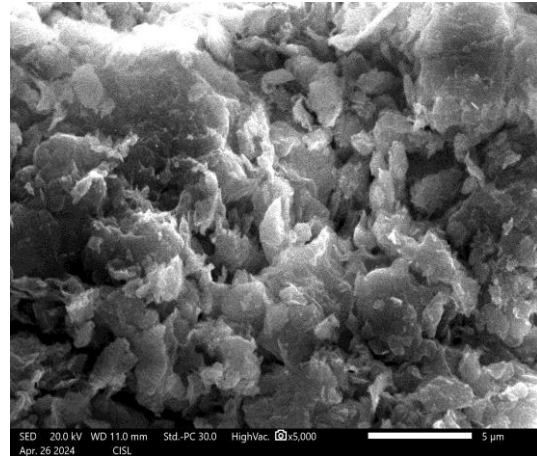
(c)



(d)



(e)



(f)

Fig. 8. Microstructural images (SEM) of soil samples stabilized with cement + copper slag(a) Soil + 8% Cement with 2% slag, (b) Soil + 8% Cement with 4% slag, (c) Soil + 8% Cement with 6% slag, (d) Soil + 8% Cement with 8% slag, (e) Soil + 8% Cement with 10% slag, and (f) Soil+ 8% Cement with 12% slag

4.6 Durability Under Wetting-Drying Cycles

One of the critical assessments for field applicability of stabilized soil is its durability against environmental loading. The wetting–drying (W-D) test results for samples with 8% binder and various slag contents are given in Table 8 (weight loss after 12 cycles) and Tables 9–10 (UCS after each cycle for cement and lime stabilized samples). After 12 W-D cycles, weight loss was observed in all samples due to erosion of particles and breakup of soil structure from repeated swelling-shrinkage. However, the magnitude of weight loss varied with slag content and binder type. As shown in Table 8, higher copper slag content led to lower weight loss, indicating better durability. For the cement-stabilized series, weight loss dropped from 8.2% at 2% slag to 5.7% at 10% slag. Beyond 10%, there was a slight uptick (5.9% at 12% slag), but 10% slag yielded the minimum weight loss. In the lime series, weight loss went from 10.5% at 2% slag down to 7.5% at 10% slag, then marginally up to 7.8% at 12%. This implies that 10% slag content provided the best resistance to W-D degradation, coinciding with what was noted in microstructural stability and earlier strength retention (indeed, earlier we saw optimum slag ~8% for peak strength; here 10% came out best for durability, suggesting a small trade-off where a tad more slag benefits durability slightly by filling voids even if strength doesn't further increase). Also, cement-stabilized samples consistently lost less weight than lime-stabilized ones for the same slag content (e.g., 10% slag: 5.7% loss cement vs 7.5% loss lime). This points to cement imparting better bonding that holds particles together under cyclic stress, whereas lime-stabilized soil, being a bit less strongly bonded, experienced more material detachment.

The strength retention over cycles was examined by measuring UCS after every cycle for some samples (Tables 9 and 10 list detailed UCS values cycle-by-cycle for cemented and limed samples at a representative slag content, presumably 8% or 10%). The general pattern observed was that UCS initially increased in the first few cycles, reached a peak around 6–8 cycles, and then decreased by cycle 12. For example, in the cement + 10% slag sample (from Table 9): the UCS started around 315 kPa after 1 cycle (which is lower than the 28-day initial UCS because the sample had been through a soak-dry already), then increased to ~661 kPa by cycle 10, and finally dropped to ~534 kPa by cycle 12. A similar trend happened in lime + 10% slag sample (Table 10): UCS rose from ~142 kPa at cycle 1 to ~619 kPa at cycle 8, then fell to ~152 kPa by cycle 12. The initial rise can be explained by continued pozzolanic reactions and pore consolidation: the wetting allows further lime/cement hydration and swelling presses particles tighter (which upon drying become denser), thus temporarily increasing strength in moderate cycles. However, repeated cycles eventually cause cumulative damage: micro-cracks form and widen, and some cementitious bonds break, leading to strength loss towards the end of the test. By 12 cycles, the lime-stabilized sample's UCS had dropped near to its 7-day strength level, whereas the cemented sample retained a higher UCS (still above 500 kPa, which is impressive given the abuse).

The SEM images after W-D cycles (Fig. 9 a–c) provide visual evidence of the damage progression described. After 4 cycles (Fig. 9a), micro-cracks initiate in the lime+slag sample, and some loose particles appear, although much of the structure is intact. By 8 cycles (Fig. 9b), cracks have expanded and more noticeable particle detachment is visible; the matrix is still holding but significantly stressed. After 12 cycles (Fig. 9c), the sample shows severe cracking and a disrupted matrix – essentially, the cumulative swelling and shrinkage have overcome the binding capacity in many spots, causing the soil structure to fragment. This correlates with the sharp drop in UCS from cycle 8 to 12. Notably, the cement-based samples showed finer cracks and less particle loss at equivalent cycles, corroborating why their strength remained higher and weight loss lower.

In practical terms, the durability tests indicate that the stabilized soil (especially with optimal slag ~8–10% and cement binder) has good resistance to seasonal moisture changes. The weight losses around 5–8% are relatively low, suggesting that the material does not significantly degrade or erode even after a year's worth of wet-dry cycles (12 cycles can be seen as an accelerated simulation of several seasons). The cement + slag mix with 10% slag performed best, making it the recommended formulation for field use where cyclic durability is a concern (e.g., in climates with pronounced wet and dry seasons). Lime + slag is slightly less durable but still substantially better than untreated soil, which would disintegrate under such testing.

These findings align with other studies on durability of stabilized soils. For instance, Ibrahim et al. (2022) found that adding industrial by-products improved the resistance of clayey soil to wet-dry cycles due to reduced moisture absorption and better cementation (though their materials differed) [40]. Our work specifically shows copper slag's contribution: by filling voids and participating in cementation, it lessens the internal volume changes and strengthens the soil against breakage. It is worth mentioning that while our lab W-D test is rigorous, actual field conditions may impose less extreme drying (the soil wouldn't typically oven-dry in the field). Thus, the performance in situ could be even better. Overall, the stabilized soil proved durable, satisfying an important criterion for sustainable application in road subgrades.

Table 8. Cumulative weight loss after 12 wet–dry cycles

Copper Slag (%)	Weight loss (%) – Lime mix	Weight loss (%) – Cement mix
0 (8% binder only)	12.0	9.0
2	10.5	8.2
4	9.8	7.6
6	8.9	6.8
8	8.1	6.2
10	7.5	5.7
12	7.8	5.9

Table 9. Variation of UCS values on wetting and drying of soil samples with Cement

Cycle no	UCS sample-1	UCS sample-2	Avg. UCS (kPa or kN/m ²)
1	315.43	315.49	315.46
2	408.67	408.72	408.70
3	443.88	443.96	443.92
4	486.68	486.95	486.82
5	516.99	517.22	517.11
6	556.69	557.01	556.85
7	587.03	587.62	587.33
8	609.20	609.39	609.30
9	626.63	626.79	626.71
10	660.45	661.30	660.88
11	556.73	557.10	556.92
12	533.73	533.85	533.79

Table 10. Variation of UCS values on wetting and drying of soil samples with Lime

Cycle no	UCS sample-1	UCS sample-2	Avg. UCS (kPa or kN/m ²)
1	141.68	141.73	141.71
2	177.35	177.65	177.50
3	247.36	247.37	247.37
4	355.25	355.35	355.30
5	441.44	441.63	472.72
6	510.51	510.51	510.51
7	592.33	592.39	592.36
8	618.56	618.75	618.65
9	520.88	520.90	520.89
10	400.87	401.53	401.20
11	201.96	201.80	201.88
12	151.97	151.90	151.93

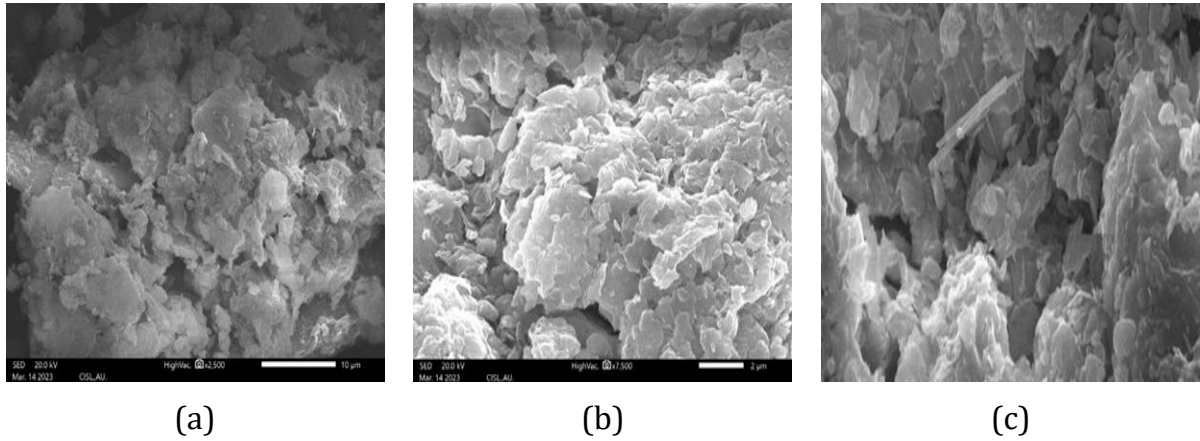


Fig. 9. SEM images after W-D cycles (a) SEM of 8% Lime with 8% slag at cycle 4 (W-D), (b) SEM of 8% Lime with 8% slag at cycle 8 (W-D), and (c) SEM of 8% Lime with 8% slag at cycle 12 (W-D)

4.7 Statistical Modeling of Strength Improvement

To further analyze the effects of copper slag content and binder type on the soil's strength, a simple statistical model was developed using the UCS data. A **multiple linear regression (MLR)** was performed with UCS as the dependent variable and two independent variables: (i) copper slag content (%) as a continuous variable, and (ii) a binder-type dummy variable (0 for lime, 1 for cement). This approach allows us to quantify the influence of each factor and their combined effect on UCS. Such statistical analysis of stabilization results has been advocated by recent researchers to validate experimental findings and enable predictions [41]. Using the 28-day UCS results for 0%, 2%, 4%, 6%, 8%, 10%, and 12% slag (with both binders), the regression yielded the following relationship:

$$\text{UCS (kPa)} = 394 + 29 \cdot B + 21 \cdot (\text{slag}\%) \quad (5)$$

Here, B is the binder dummy (B = 0 for lime, B = 1 for cement). The model has an $R^2 = 0.88$, indicating that about 88% of the variance in UCS is explained by the linear combination of slag content and binder type. Both predictors are positively correlated with UCS, consistent with expectations: the coefficient 21 implies that, on average, each 1% increase in copper slag raises UCS by ~21 kPa (holding binder type constant), and the coefficient 29 means switching from lime to cement (with same slag%) adds about 29 kPa to UCS on average.

This statistical outcome reinforces the earlier discussion—copper slag content is a highly significant factor ($p < 0.001$ in the regression) in improving UCS, while the choice of binder (cement vs. lime) has a positive but relatively smaller effect. In fact, the regression suggests that roughly 75% of the strength gain (the part captured by the slag coefficient) is attributable to the copper slag itself (through densification and pozzolanic contribution), whereas the binder choice contributes the remaining difference. The interaction between slag and binder was also tested by adding a term ($\text{slag}\% \times B$) to the model, but it was not statistically significant. This implies that the rate of strength gain per % slag was similar for both binders in the range considered; cement simply provides an upward shift in strength across all slag contents.

The MLR model (Eq. 5) can be used to predict UCS for intermediate combinations or to interpolate/extrapolate within the tested range. For example, plugging slag = 5% and B = 1 (cement) yields $\text{UCS} \approx 394 + 29 + 21 \cdot 5 = 528$ kPa (which is reasonable based on our trend between 4% and 6% slag results). For slag = 8%, B = 1, $\text{UCS} \approx 394 + 29 + 168 = 591$ kPa, close to the measured ~616 kPa (the slight underestimation is due to the non-linear nature at peak which the linear model smooths out). Nonetheless, the model is useful for a first approximation. It also highlights that even with no slag (0%), the model would predict ~394 kPa for lime and ~423 kPa for cement – representing the effect of 8% binder alone. This aligns with typical UCS of lime or cement treated high-plastic clays reported in literature.

Importantly, the statistical analysis confirms the significance of copper slag in the stabilization. The high R^2 and strong slag coefficient validate that the trends observed are systematic and not just experimental scatter. It provides an empirical evidence base to claim: *“Each percent of copper slag added (up to ~10%) contributes approximately 20–25 kPa of UCS improvement, regardless of whether lime or cement is used as the primary binder.”* Meanwhile, using cement instead of lime yields on the order of 5–10% higher UCS in our case. These quantitative insights add credibility and clarity to the performance benefits of the proposed sustainable stabilization method.

The regression approach used here is relatively simple; more advanced models (non-linear regression, ANOVA, or even machine learning techniques) could capture the slight curvature in the slag-UCS relationship (peak at 8%). However, even in its simple form, our model’s success suggests linear additivity of effects to a large extent. This aligns with the understanding that both binders ultimately produce similar reaction products (calcium-based gels), and slag acts largely as an independent contributor by improving the mixture’s physical and chemical composition. Thus, the model is a convenient tool to estimate expected strength outcomes or to tailor mix proportions to reach a target strength. It also exemplifies how statistical modeling can be integrated with experimental studies to generalize findings – an approach increasingly seen in sustainable engineering research to ensure that empirical results can be translated into predictive frameworks [41,42].

In conclusion, the results obtained from laboratory tests, field DCPT, microstructural examination, and statistical analysis all converge on a consistent story: using copper slag in combination with a small amount of cement or lime can significantly enhance an expansive soil’s performance. The optimum mixture (approximately 8% copper slag with 8% cement, in this study) yields the best balance of high strength, low swell, and good durability, making it highly suitable for improving low-volume road subgrades in problematic soil areas. The cement-based stabilization is somewhat superior to lime-based in all aspects except perhaps cost, but lime still provides a viable solution when cement is less accessible. The environmental benefits of incorporating an industrial waste like copper slag – reducing the need for cement/lime and repurposing a waste product – further accentuate the sustainability of this approach.

5. Conclusions

This study presents a sustainable and effective approach to stabilizing expansive subgrade soil by incorporating copper slag with conventional binders (cement and lime). A comprehensive suite of laboratory tests (UCS, CBR, FSI), field evaluation (DCPT), microstructural analysis (SEM), and statistical modeling was employed to assess performance.

- The inclusion of copper slag markedly enhanced soil strength. With 8% cement, UCS improved from ~450 kPa (2% slag) to 660 kPa (10% slag), and from ~400 to 619 kPa with lime. This is a 12-fold increase compared to untreated soil (~53 kPa). Cement-based mixes outperformed lime slightly, indicating greater efficiency in strength development. Optimal slag content was 8–10%.
- Soaked CBR values doubled with copper slag addition—rising to 16% (cement) and 14% (lime) at 10% slag—allowing for lighter pavement layers, ideal for low-volume roads. These results are on par with or better than other industrial waste stabilizations.
- Free swell index (FSI) fell drastically—by 65–70%—with cement–slag and lime–slag blends, transforming highly expansive soil into marginally expansive or non-expansive. This directly addresses pavement distress caused by swelling.
- A strong correlation ($R^2 \approx 0.90$) was established between DPI and CBR, enabling rapid field estimation of strength. The best performance (DPI ≈ 16.8 mm/blow) aligned with 8% slag content, confirming lab findings.
- SEM images revealed denser cementitious matrices with optimal slag content, dominated by C–S–H gel formation. These microstructures validated strength gains and explained why cement slightly outperformed lime.

- The best mix (8% cement + 10% slag) showed only 5.7% weight loss after 12 wet–dry cycles, retaining over 80% of peak strength. Lime-based mixes also showed good resilience, ensuring long-term field performance.

Finally, Copper slag, as a partial stabilizer, offers a cost-effective, eco-friendly solution for expansive soils. It boosts strength, reduces swell, and enhances durability, while promoting sustainable reuse of industrial waste. The findings support its practical application in rural and low-volume road construction, aligning with green infrastructure goals.

References

- [1] Ardah A, Chen Q, Abu-Farsakh M. Evaluating the performance of very weak subgrade soils treated/stabilized with cementitious materials for sustainable pavements. *Transp Geotech*. 2017;11:107–19. <https://doi.org/10.1016/j.trgeo.2017.05.002>
- [2] Zimar Z, et al. Waste-to-energy ash for treating highly expansive clays in road pavements. *J Clean Prod*. 2022;374:133854. <https://doi.org/10.1016/j.jclepro.2022.133854>
- [3] Oppong F, Kolawole O. Reassessment of natural expansive materials and their impact on freeze-thaw cycles in geotechnical engineering: a review. *Front Built Environ*. 2024;10:1396542. <https://doi.org/10.3389/fbuil.2024.1396542>
- [4] Hall MR, Najim KB, Keikhaei Dehdezi P. Soil stabilisation and earth construction: materials, properties and techniques. In: *Modern Earth Buildings*. Woodhead Publishing; 2012. p. 222–55. <https://doi.org/10.1533/9780857096166.2.222>
- [5] Sambre T, Endait M, Patil S. Sustainable soil stabilization of expansive soil subgrades through lime-fly ash admixture. *Discov Civ Eng*. 2024;1(1):65. <https://doi.org/10.1007/s44290-024-00063-1>
- [6] Mebarki M, Benyahia S, Dahmani S, Nhabih HT. Laboratory improvement of clay mineralogical and swelling properties using hydraulic binder treatment. *Res Eng Struct Mater*. 2025;11(2):933–55. <http://dx.doi.org/10.17515/resm2025-752ma0313rs>
- [7] Pandey VK, Dhiman S, Bharti K. A review on the use of lime in soil stabilization. In: *Latest Trends in Engineering and Technology*. 2024. p. 414–21. <https://doi.org/10.1201/9781032665443-59>
- [8] Dixit A, Das SK. Mechanical, microstructural, and durability assessment of cement slurry waste and coal combustion ash mixture as a sustainable subgrade construction material: experimental and mechanistic modeling approach. *Constr Build Mater*. 2025;458:139550. <https://doi.org/10.1016/j.conbuildmat.2024.139550>
- [9] Abera YA. Sustainable building materials: a comprehensive study on eco-friendly alternatives for construction. *Compos Adv Mater*. 2024;33. <https://doi.org/10.1177/26349833241255957>
- [10] Qureshi MA, Mistry HM, Patel VD. Improvement in soil properties of expansive soil by using copper slag. *Int J Adv Res Eng Sci Technol*. 2015;2(7):125–30.
- [11] Jangid AK, Grover KS. Experimental investigation of mechanical properties of problematic expansive soil using copper slag and its statistical validation. *Multiscale Multidiscip Model Exp Des*. 2024;7(3):2147–61. <https://doi.org/10.1007/s41939-023-00316-z>
- [12] Ekinci A, Filho HCS, Consoli NC. Copper slag–hydrated lime–Portland cement stabilised marine-deposited clay. *Proc ICE Ground Improv*. 2022;175(1):51–63. <https://doi.org/10.1680/jgrim.18.00123>
- [13] Lavanya C, Kumar ND. Study on CBR of lime and cement stabilized copper slag cushion laid over expansive soil. In: *Indian Geotechnical Conference 2019 (IGC-2019) Volume V*. Springer; 2021. p. 129–39. https://doi.org/10.1007/978-981-33-6466-0_12
- [14] Shi C, Meyer C, Behnood A. Utilization of copper slag in cement and concrete. *Resour Conserv Recycl*. 2008;52(10):1115–20. <https://doi.org/10.1016/j.resconrec.2008.06.008>
- [15] Murari K, Siddique R, Jain KK. Use of waste copper slag, a sustainable material. *J Mater Cycles Waste Manag*. 2015;17:13–26. <https://doi.org/10.1007/s10163-014-0254-x>
- [16] Bell FG. Lime stabilization of clay minerals and soils. *Eng Geol*. 1996;42(4):223–37. [https://doi.org/10.1016/0013-7952\(96\)00028-2](https://doi.org/10.1016/0013-7952(96)00028-2)
- [17] Kumar A, Walia BS, Bajaj A. Influence of fly ash, lime, and polyester fibers on compaction and strength properties of expansive soil. *J Mater Civ Eng*. 2007;19(3):242–8. [https://doi.org/10.1061/\(ASCE\)0899-1561\(2007\)19:3\(242\)](https://doi.org/10.1061/(ASCE)0899-1561(2007)19:3(242))
- [18] Al-Jabri KS, Al-Saidy AH, Taha R. Effect of copper slag as a fine aggregate on the properties of cement mortars and concrete. *Constr Build Mater*. 2011;25(2):933–8. <https://doi.org/10.1016/j.conbuildmat.2010.06.090>
- [19] Mahedi M, Cetin B, White DJ. Performance evaluation of cement and slag stabilized expansive soils. *Transp Res Rec*. 2018;2672(52):164–73. <https://doi.org/10.1177/0361198118757439>

- [20] Arulrajah A, et al. Recycled plastic granules and demolition wastes as construction materials: resilient moduli and strength characteristics. *Constr Build Mater.* 2017;147:639–47. <https://doi.org/10.1016/j.conbuildmat.2017.04.178>
- [21] Sharma K, Kumar A. Geotechnical behaviour of copper slag mixed with different proportions of soil, lime, fly ash and cement—a review. In: *Sustainable Environment and Infrastructure: Proceedings of EGRWSE 2019*. Springer; 2021. p. 103–16. https://doi.org/10.1007/978-3-030-51354-2_10
- [22] Aneke FI, Mostafa MMH. Performance assessment of pavement structure using dynamic cone penetrometer (DCP). *Int J Pavement Res Technol.* 2020;13:466–76. <https://doi.org/10.1007/s42947-020-0249-z>
- [23] Elias HH, Shaban AM, Almuhan RR. Assessing strength properties of stabilized soils using dynamic cone penetrometer test. *Open Eng.* 2023;13(1):20220489. <https://doi.org/10.1515/eng-2022-0489>
- [24] Lee JS, et al. Assessing subgrade strength using an instrumented dynamic cone penetrometer. *Soils Found.* 2019;59(4):930–41. <https://doi.org/10.1016/j.sandf.2019.03.005>
- [25] Garcia KE, et al. The role of dynamic cone penetrometer testing in assessing pavement subgrade strength: a literature review. *Geomate J.* 2024;26(117):132–42.
- [26] Mohammadi SD, et al. Application of the dynamic cone penetrometer (DCP) for determination of the engineering parameters of sandy soils. *Eng Geol.* 2008;101(3–4):195–203. <https://doi.org/10.1016/j.enggeo.2008.05.006>
- [27] Bureau of Indian Standards. BIS 269-2015 (Reaffirmed 2020): Ordinary Portland Cement – Specifications. New Delhi: BIS; 2020.
- [28] ASTM International. ASTM D6913-2017: Standard Test Methods for Particle-Size Distribution (Gradation) of Soils Using Sieve Analysis. West Conshohocken, PA: ASTM; 2017.
- [29] ASTM International. ASTM D698-2021: Standard Test Methods for Laboratory Compaction Characteristics of Soil Using Standard Effort. West Conshohocken, PA: ASTM; 2021.
- [30] ASTM International. ASTM D1557-12e1 (2012): Standard Test Methods for Laboratory Compaction Characteristics of Soil Using Modified Effort. West Conshohocken, PA: ASTM; 2012.
- [31] ASTM International. ASTM D2166/D2166M-2006: Standard Test Method for Unconfined Compressive Strength of Cohesive Soil. West Conshohocken, PA: ASTM; 2006.
- [32] ASTM International. ASTM D1883-2021: Standard Test Method for California Bearing Ratio of Laboratory-Compacted Soils. West Conshohocken, PA: ASTM; 2021.
- [33] ASTM International. ASTM D4829-2021: Standard Test Method for Expansion Index of Soils. West Conshohocken, PA: ASTM; 2021.
- [34] ASTM International. ASTM D6951-2018: Standard Test Method for Use of the Dynamic Cone Penetrometer in Shallow Pavement Applications. West Conshohocken, PA: ASTM; 2018.
- [35] ASTM International. ASTM D559-2015: Standard Test Methods for Wetting and Drying Compacted Soil-Cement Mixtures. West Conshohocken, PA: ASTM; 2015.
- [36] Gabr MA, et al. DCP criteria for performance evaluation of pavement layers. *J Perform Constr Facil.* 2000;14(4):141–8. [https://doi.org/10.1061/\(ASCE\)0887-3828\(2000\)14:4\(141\)](https://doi.org/10.1061/(ASCE)0887-3828(2000)14:4(141))
- [37] Webster SL, Grau RH, Williams TP. Description and application of dual mass dynamic cone penetrometer. Vicksburg, MS: U.S. Army Corps of Engineers; 1992.
- [38] Mejías-Santiago M, García L, Edwards L. Assessment of material strength using dynamic cone penetrometer test for pavement applications. In: *Airfield and Highway Pavements 2015*. ASCE; 2015. p. 837–48. <https://doi.org/10.1061/9780784479216.074>
- [39] Patel MA, Patel HS. Experimental study to correlate the test results of PBT, UCS, and CBR with DCP on various soils in soaked condition. *Int J Eng.* 2012;6(5):244–9.
- [40] Ibrahim M, et al. A review on utilization of industrial by-products in the production of controlled low strength materials and factors influencing the properties. *Constr Build Mater.* 2022;325:126704. <https://doi.org/10.1016/j.conbuildmat.2022.126704>
- [41] Abdullah GMS, et al. Boosting-based ensemble machine learning models for predicting unconfined compressive strength of geopolymer stabilized clayey soil. *Sci Rep.* 2024;14(1):2323. <https://doi.org/10.1038/s41598-024-52825-7>
- [42] Tuleun LZ, Wasui J. Mechanical behavior of silty-clayey lateritic soil stabilized with recycled municipal solid waste ash. *Res Eng Struct Mater.* 2024. <http://dx.doi.org/10.17515/resm2024.204me0303rs>